DE GRUYTER Current Directions in Biomedical Engineering 2016; 2(1): 715–718

Open Access

David Graurock, Thomas Schauer and Thomas Seel*

Automatic pairing of inertial sensors to lower limb segments – a plug-and-play approach

DOI 10.1515/cdbme-2016-0155

Abstract: Inertial sensor networks enable realtime gait analysis for a multitude of applications. The usability of inertial measurement units (IMUs), however, is limited by several restrictions, e.g. a fixed and known sensor placement. To enhance the usability of inertial sensor networks in every-day live, we propose a method that automatically determines which sensor is attached to which segment of the lower limbs. The presented method exhibits a low computational workload, and it uses only the raw IMU data of 3 s of walking. Analyzing data from over 500 trials with healthy subjects and Parkinson's patients yields a correct-pairing success rate of 99.8% after 3 s and 100% after 5 s.

Keywords: automatic calibration; inertial sensor networks; realtime gait analysis; sensor-to-segment pairing; wireless inertial measurement units.

1 Introduction

Miniature inertial sensors are a novel and promising technology that allows precise assessment of human motion in clinical environments. However, for most systems each sensor has to be attached to a predefined body segment and often with a predefined sensor-to-segment orientation. Therefore, the set-up of the inertial systems is time-consuming and prone to errors if not supervised by a qualified instructor. This impedes the use of inertial sensors for home care systems, daily-life assistive devices and long-term motion analysis. In a multitude of clinical applications, it is desirable to let the patient attach the sensors autonomously and to employ a method that automatically determines which sensor has been attached to which body segment.

In particular, the following problem must be solved: Assume that six inertial sensor are attached to the lower limbs as depicted in Figure 1. Assume furthermore that it is not known which sensor has been attached to which of the six segments, nor in which orientation it has been attached. As the subject moves, the sensor readings should be used to determine which sensor are attached to the feet, to the shanks and to the thighs, and which are attached to the one side of the body and which to the other. This shall be achieved without requiring a specifically precise motion or posture.

Several methods have been proposed, which might be employed to solve this problem. [1] and [2] introduced methods for recognizing the on-body position of a sensor during walking. To this end, they use machine-learning methods and a large training set. Weenk et al. [3] presented a method for automatic identification of the sensor positions during walking for a full-body setup of 17 inertial sensors. This method relies on inertial sensor orientation estimation, which is besides its computational cost an error-prone procedure. In addition they require the subject to stand still in the beginning. Lambrecht et al. [4] developed a computationally low-cost method for the sensor position identification on the upper limbs that relies on special motions which the user has to perform.

We propose a method for the *sensor-to-segment pairing* on the lower limbs that aims for a low computational workload and supersedes the need for precise postures or movements. In particular, we

- only assume the user to be walking,
- use the raw accelerometer and gyroscope readings,
- identify the paring from only 3 s of walking,
- require no computationally expensive computations.

2 Method

Consider the setup depicted in Figure 1. Assume that each IMU provides 3D accelerometer readings $\mathbf{a}(t)$ as well as 3D gyroscope readings $\mathbf{g}(t)$ at a measurement sampling interval of $t_s = 0.02$ s. Since we have no prior knowledge about the sensor-to-segment orientations, we only use the

***Corresponding author: Thomas Seel,** Control Systems Group, Technische Universität Berlin, Germany, E-mail: seel@control.tu-berlin.de
David Graurock and Thomas Schauer: Control Systems Group, Technische Universität Berlin, Germany

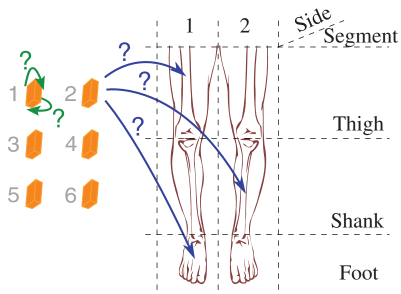

Figure 1: Definition of the different sensor positions, which are used for the proposed sensor-to-segment pairing method.

Euclidean norms of the measured vectors. To minimize the influence of signal fluctuation, we always apply sufficient low-pass filtering to these norm signals. We denote the low-pass filtered norms by

$$\tilde{a}_i(t) = \frac{1}{20}\sum_{k=-9}^{10} ||\mathbf{a}_i(t + kt_s)||_2 - 9.8, \tag{1}$$

$$\tilde{g}_i(t) = \frac{1}{20}\sum_{k=-9}^{10} ||\mathbf{g}_i(t + kt_s)||_2, \tag{2}$$

$$\tilde{j}_i(t) = \frac{1}{20}\sum_{k=-9}^{10} \left|\left|\frac{\mathbf{a}_i(t+kt_s)-\mathbf{a}_i(t+kt_s-t_s)}{t_s}\right|\right|_2. \tag{3}$$

We denote the six sensors by an arbitrary but fixed enumeration $i \in \mathbb{S}$, $\mathbb{S} := \{1, \dots, 6\} \in \mathbb{N}$. Furthermore, we define six locations (p,s) consisting of a segment position $p \in \{\text{thigh, shank, foot}\}$ and a side $s \in \{\text{side 1, side 2}\}$.

The final goal is to assign every sensor number i to a location (p,s). E.g. we use the notation $S^{(\text{shank, side 1})} = 2$ to indicate that the shank sensor of side 1 was found to be the sensor with number $i = 2$.

In order to achieve this goal, we divide this task by its dimensions. To this end, we define sets $\mathbb{S}^{\text{foot}}$, $\mathbb{S}^{\text{shank}}$ and $\mathbb{S}^{\text{thigh}}$, each containing two sensors, such that

$$\mathbb{S}^{\text{foot}} \cup \mathbb{S}^{\text{shank}} \cup \mathbb{S}^{\text{thigh}} = \mathbb{S},$$

$$\mathbb{S}^{\text{foot}} \cap \mathbb{S}^{\text{shank}} = \mathbb{S}^{\text{foot}} \cap \mathbb{S}^{\text{thigh}} = \mathbb{S}^{\text{shank}} \cap \mathbb{S}^{\text{thigh}} = \emptyset.$$

To keep the mathematical notations short, we define an operator that returns the sensor number i of the sensor that is associated with the k^{th}-largest entry of a given set of real values.

Definition 1. *Let $\mathbf{c} \in \mathbb{R}^n$ be a set of n real values, each of which is uniquely associated with one sensor, and let $l \in \{1, 2, \dots, n\} \subset \mathbb{N}$ be a natural number. Then the operator $\langle \mathbf{c} \rangle_l \colon \mathbb{R}^n \times \{1, 2, \dots, n\} \to \{1, \dots, 6\}$ returns the sensor number of the sensor to which the l^{th}-largest entry of the set $\mathbf{c}$ is associated.*

For example, let the set $c = \{1.2, 0.3, 4.8\}$ contain the angular rate norms of sensors $i = 4, 6, 5$. Then $\langle \mathbf{c} \rangle_2 = 4$.

In order to find robust criteria for the sensor-to-segment pairing, we only consider relative comparisons of characteristic signal values, since absolute values and thresholds typically change with gait velocity as well as from subject to subject.

We analyzed a large number of characteristics and features in the signals recorded during gait. For the sake of brevity, we present only the most useful and robust features in the present contribution. The proposed sensor-to-segment pairing algorithm consists of the following steps:

1. Identification of the *foot* sensors
2. Identification of the *shank* and *thigh* sensors
3. Pairing the *shank* sensors to their related *foot* sensors
4. Pairing the *thigh* sensors to their related *foot* sensors

All of these steps shall be performed by processing the IMU measurements that are collected during 3 s of gait. Let $t_0 \in \mathbb{R}^{\geq 0}$ be the start point and $t_f > t_0 \in \mathbb{R}^{\geq 0}$ be the end point of the data collection.

With respect to Step 1, consider the following feature:

Feature 1: *Foot sensors have the highest all-time-maximum of low-pass-filtered acceleration.*

Note that the *all-time-maximum* is the maximum over the 3 s of collected data.
To exploit this feature, we define a set $\tilde{\mathbf{a}}_{\max} \in \mathbb{R}^6$ with

$$\tilde{\mathbf{a}}_{\max} := \{\max_{t \in \{t_0, \dots, t_f\}} \tilde{a}_i(t), i \in \mathbb{S}\} \tag{4}$$

$$\Rightarrow \quad \mathbb{S}^{\text{foot}} = \{\langle \tilde{\mathbf{a}}_{\max} \rangle_1, \langle \tilde{\mathbf{a}}_{\max} \rangle_2\}. \tag{5}$$

Once we know the *foot* sensors, the *shank* and *thigh* are distinguished by exploiting the following feature:

Feature 2: *Shank sensors have higher all-time-maximum of low-pass-filtered angular rates than thigh sensors.*

We exploit this feature by defining a set $\tilde{\mathbf{g}}_{\max} \in \mathbb{R}^4$ with

$$\tilde{\mathbf{g}}_{\max} = \{\max_{t \in \{t_0, \dots, t_f\}} \tilde{g}_i(t), i \in \mathbb{S} \setminus \mathbb{S}^{\text{foot}}\} \tag{6}$$

$$\Rightarrow \quad \mathbb{S}^{\text{shank}} = \{\langle \tilde{\mathbf{g}}_{\max} \rangle_1, \langle \tilde{\mathbf{g}}_{\max} \rangle_2\}. \tag{7}$$

Once we know the *foot* and *shank* sensors, we consequently know the *thigh* sensors:

$$\mathbb{S}^{\text{thigh}} = \mathbb{S} \setminus (\mathbb{S}^{\text{foot}} \cup \mathbb{S}^{\text{shank}}). \tag{8}$$

For Step 3 and 4, we must identify the sides. Without prior knowledge, we have no means to distinguish both legs in terms of *left* and *right*. Note that one might assume that both feet exhibit more inversion than eversion or that

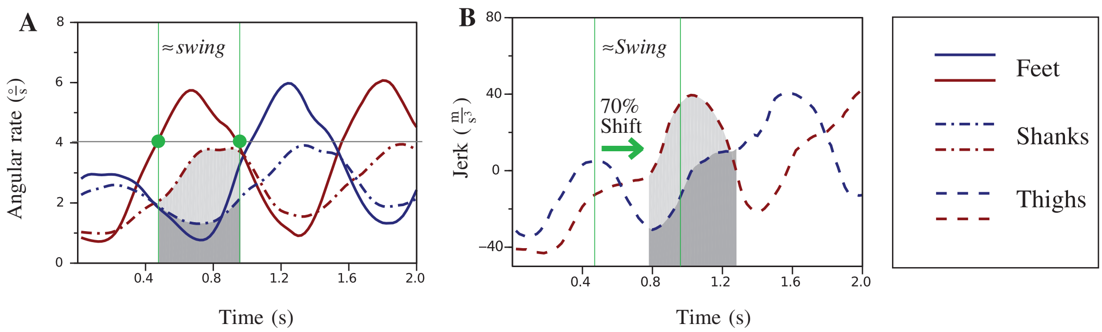

Figure 2: (A) Low-pass-filtered angular rates for one foot sensor and both shank sensors. Green dots indicate when the angular rate of the foot rises/falls above/below the all-time maximum angular rate (horizontal line) of both shank sensors. These events define the beginning and the end of the approximate swing phase (vertical lines). Integrating the signals over this time interval allows evaluation of Feature 3. (B) Low-pass-filtered zero-mean jerk of both thigh sensors. The integration interval that is used for evaluation of Feature 4 is shifted by 70% of $T_{\approx swing}$ as indicated by the green arrow.

both thighs exhibit more abduction than adduction during swing phase. However, these assumptions might easily be violated in pathological gaits. Therefore, we refrain from assuming any of such assumptions. Instead, we let the two *foot* sensors represent one leg each. Thus, we must find out which *shank* and *thigh* sensor belongs to which of the two *foot* sensors, in the following.

This goal is achieved by exploiting some fundamental characteristics of gait: In general, gait means that both legs alternate between stance and swing. During swing, both the *shank* and the *foot* of the swinging leg rotate quickly. Let us approximate the swing phase of one leg by the period of time in which the angular rate of the *foot* sensor is higher than the all-time maximum angular rate of both *shank* sensors. We denote the duration of this time interval by $T_{\approx swing}$.

> ***Feature 3****: During swing phase of one leg, the shank sensor of that leg measures a higher low-pass-filtered angular rate than the other shank sensor (see Figure 2a).*

Denote the side of the leg that undergoes the first swing-phase (within the collected data) by side 1 and assign the foot sensors to the sides 1 and 2 accordingly. We compare the integrals of both angular rates of the *shank* sensors during $T_{\approx swing}$. Define $G^{\text{shank}} \in \mathbb{R}^2$, with $G^{\text{shank}} = \{\int_{T_{\approx swing}} \tilde{g}_i(t)\,\mathrm{d}t, i \in \mathbb{S}^{\text{shank}}\}$. Then

$$S^{(\text{shank,side1})} = \langle G^{\text{shank}} \rangle_1, \tag{9}$$

$$S^{(\text{shank,side2})} = \mathbb{S}^{\text{shank}} \setminus S^{(\text{shank,side1})}. \tag{10}$$

For the final step of pairing a *thigh* sensor to its related *foot* sensor, the zero-mean jerk

$$\tilde{j}_i(t) = \tilde{j}_i(t) - \tfrac{1}{t_f - t_0} \int_{t_0}^{t_f} \tilde{j}_i(t)\mathrm{d}t \tag{11}$$

was found to be a useful signal. Just like the angular rates for *foot* and *shank* sensors, the jerk of the *thigh* sensors alternates between high phases and low phases. These high-*thigh*-jerk phases appear a little later than the (approximated) swing phases of the corresponding foot. We quantify this time-shift to be approximately 70% of the swing duration $T_{\approx swing}$ and denote it by $\hat{T}_{\approx swing}$.

> ***Feature 4****: Near the end of the swing phase of one leg, the thigh sensor of that leg measures a higher low-pass-filtered zero-mean jerk than the other thigh sensor.*

For illustration, see Figure 2b. We define $J^{\text{thigh}} \in \mathbb{R}^2$ with $J^{\text{thigh}} = \{\int_{\hat{T}_{\approx swing}} \tilde{j}_i(t)\,\mathrm{d}t, i \in \mathbb{S}^{\text{thigh}}\}$. Then

$$S^{(\text{thigh,side1})} = \langle J^{\text{thigh}} \rangle_1, \tag{12}$$

$$S^{(\text{thigh,side2})} = \mathbb{S}^{\text{thigh}} \setminus S^{(\text{thigh,side1})}. \tag{13}$$

3 Experimental results

In order to evaluate the reliability of the proposed sensor-to-segment pairing, we analyze the data of three different experiments with several subjects and walking-trials. In all trials, the subjects were equipped with the proposed setup of six IMUs on the lower limbs. All subjects walked on a straight line at either slow, medium (self-selected) or fast pace. We analyzed 85 walking-trials of five healthy subjects, 53 trials of six ambulatory elderly patients suffering from Parkinson's disease (partially with walking frame) and 395 trials of eleven healthy barefoot walking subjects, who walked at slow, normal and fast pace with two additional inertial sensors on the right thigh.

Table 1 presents the results of the sensor-to-segment pairings. Please note that only a correct classification of *all* six sensors was counted as a successful trial.

Table 1: Success rate of the sensor-to-segment pairing.

Speed	16 Subjects Slow	Medium	Fast	6 Patients self assessed
Trials	132	216	132	53
Pairing	**99.2%**	**100%**	**100%**	**100%**

Table 2: Influence of thigh sensor placement.

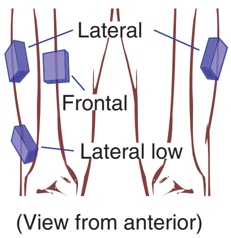

Sensor Position	Pairing success
Lateral	99.7%
Frontal	99.5%
Lateral low	100.0%
Average	**99.7%**

A classification rate of 532 out of 533 trials is achieved for all subjects including fast and slow walkers as well as barefoot and shoe walkers and even Parkinson patients.

In Table 2 we see the results of the sensor-to-segment pairing for different thigh sensor positions. While the left thigh sensor is always attached to the *lateral* position, three positions (*lateral*, *lateral low* and *frontal*) are considered for the right thigh sensor. Even for the two asymmetric mountings, the classification rate remains very close to 100%.

In clinical applications, a reliability of 100% is obligatory. In order to achieve this perfect rate, we propose an online implementation of the presented method, such that it is applied repeatedly during walking. More precisely, we continuously store the data of the last 3 s in a ringbuffer and apply the proposed method to that data every second. Consequently, we obtain three paring results within the first 5 s, five pairing results within the first 7 s, and so on. At all times, if conflicting results are obtained, the algorithm only returns the most frequent sensor-to-segment pairing result. Using the same data as before, the online implementation achieves a success rate of 100% after 5 s already, i.e. the sensor-to-segment pairing is always correctly identified from at most three executions of the presented algorithm.

4 Conclusion

The results demonstrate that the sensor-to-segment pairing is highly reliable under a multitude of different conditions. In particular, neither the different walking styles and velocities nor the sensor placement had an influence on the pairing success of **100%** after 5 s. We conclude that the proposed method enhances the practical usability of IMU-based gait analysis in many clinical applications. The user can independently attach the inertial sensors without the need for professional supervision. Since we refrained from using magnetometer readings, the methods are highly suitable for indoor environments. Our present and future work focuses on the combination of the presented method and methods for inertial gait analysis [5–7] to realize a plug-and-play gait analysis system.

Acknowledgment: We would like to express our deep gratitude to Noelia Chia Bejarano and Simona Ferrante from Politecnico di Milano as well as to Gunnar Leivseth from NTNU Trondheim who provided some of the datasets that were analyzed.

Author's Statement

Research funding:This work was supported by the German Federal Ministry of Education and Research (FKZ 16SV7069K). Conflict of interest: Authors state no conflict of interest. Material and Methods: Informed consent: Informed consent has been obtained from all individuals included in this study. Ethical approval: The research related to human use complies with all the relevant national regulations, institutional policies and was performed in accordance with the tenets of the Helsinki Declaration, and has been approved by the authors' institutional review board or equivalent committee.

References

[1] Kunze K, Lukowicz P, Junker H, Tröster G. Where am I: recognizing on-body positions of wearable sensors. Location- and Context-Awareness, Volume 3479 of Lecture Notes in Computer Science, Springer, 2005:264–75.
[2] Mannini A, Sabatini AM, Intille SS. Accelerometry-based recognition of the placement site of a wearable sensor. Pervasive Mobile Comp. 2015;21:62–74.
[3] Weenk D, van Beijnum B, Baten C, Hermens H, Veltink P. Automatic identification of intertial sensor placement on human body segments during walking. J NeuroEng Rehabil. 2013;10:31.
[4] Lambrecht S, Romero JP, Benito-Leon J, Rocon E, Pons JL. Task independent identification of sensor location on upper limb from orientation data. Engineering in Medicine and Biology Society, 36th Annual International Conference of the IEEE, 2014;6627–30.
[5] Seel T, Landgraf L, Víctor Cermeño Escobar, Raisch J, Schauer T. Online gait phase detection with automatic adaption to gait velocity changes using accelerometers and gyroscopes. Biomed Eng. 2014;59:795–8.
[6] Seel T, Graurock D, Schauer T. Realtime assessment of foot orientation by accelerometer and gyroscopes. Curr Dir Biomed Eng 2015;1:466–9.
[7] Seel T, Schauer T, Raisch J. IMU-based joint angle measurement for gait analysis. Sensors. 2014;14:6891–909.